ACS APPLIED MATERIALS & INTERFACES

Letter

www.acsami.org

# Low Ice Adhesion on Nano-Textured Superhydrophobic Surfaces under Supersaturated Conditions

Srinivas Bengaluru Subramanyam,[†] Vitaliy Kondrashov,[§] Jürgen Rühe,[§] and Kripa K. Varanasi*[,‡]

[†]Department of Materials Science and Engineering and [‡]Department of Mechanical Engineering, Massachusetts Institute of Technology, Cambridge, Massachusetts 02139, United States

[§]Department of Microsystems Engineering - IMTEK, Chemistry and Physics of Interfaces, University of Freiburg, 79110 Freiburg, Germany

Supporting Information

**ABSTRACT:** Ice adhesion on superhydrophobic surfaces can significantly increase in humid environments because of frost nucleation within the textures. Here, we studied frost formation and ice adhesion on superhydrophobic surfaces with various surface morphologies using direct microscale imaging combined with macroscale adhesion tests. Whereas ice adhesion increases on microtextured surfaces, a 15-fold decrease is observed on nanotextured surfaces. This reduction is because of the inhibition of frost formation within the nanofeatures and the stabilization of vapor pockets. Such "Cassie ice"-promoting textures can be used in the design of anti-icing surfaces.

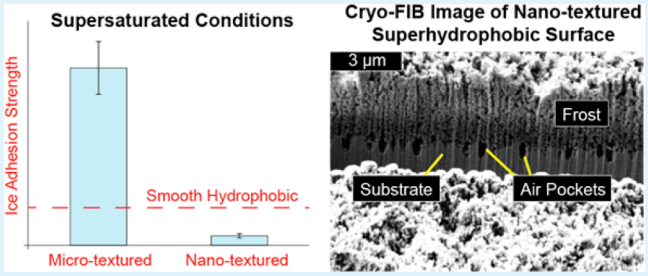


**KEYWORDS:** *ice adhesion, frost formation, nanotexture, microtexture, cryogenic imaging, cryo-FIB, cryo-SEM*

The problem of excessive ice buildup is prevalent in many systems, including airplanes, freezers, wind turbines, and power lines.[1] The current mechanical and thermal methods of ice removal and prevention are energy intensive,[2] and chemicals like deicing and anti-icing fluids are not always compatible with the environment.[3] To this end, developing passive anti-icing surfaces is of utmost importance. Over the years, solid low surface energy coatings,[4] textured surfaces with a modified surface chemistry (superhydrophobic surfaces)[5,6] and lubricant-impregnated textured surfaces[7,8] have garnered significant attention as potential approaches to prevent excessive ice accretion.

It has been reported previously that superhydrophobic surfaces repel bouncing water drops at subzero temperatures,[9,10] promote freezing delay,[11−14] and reduce ice adhesion.[5,15] This performance is attributed to water being in the Cassie state and not in the Wenzel state.[16] It has been argued that under subzero temperatures, the anti-icing properties of superhydrophobic surfaces are compromised if the substrate temperature is below the dew point.[17,18] In other words, an increase in local humidity results in the nucleation of frost within the surface features and renders the surface hydrophilic. On such frosted surfaces, the higher water wettability results in the impalement of water. Subsequent freezing of water results in ice being in intimate contact with the surface asperities, which we refer to as "Wenzel ice".[17] Surfaces where frost does not form within the surface features can sustain the Cassie state of water during freezing even under supersaturated conditions. The ice in this suspended state, which we refer to as "Cassie ice", will adhere poorly to the substrate because of reduced ice-substrate contact area. However, there has been no direct evidence of "Cassie ice" under supersaturated conditions.

Frost formation has been the subject of intensive studies in the past few years.[19−23] Here, we performed frosting experiments on superhydrophobic surfaces with varied surface textures. Figure 1 shows the experimental observations on four different silicon surfaces: a smooth surface (Figure 1a), a surface with photolithographically patterned square micropillars of 10 $\mu$m side, 10 $\mu$m spacing, and 10 $\mu$m depth (microtextured, Figure 1c), a surface with nanofeatures obtained via reactive ion etching (nanotextured, Figure 1e), and a hierarchically textured surface with 10 $\mu$m square micropillars, 10 $\mu$m spacing, and 10 $\mu$m depth along with nanofeatures (Figure 1g). All surfaces were modified with tricholoro(octadecyl)silane to make them hydrophobic. The experimental details of the sample fabrication are found elsewhere.[7,24] Table 1 shows the dynamic water contact angles on these surfaces. The substrates were placed on a cold plate (Stir-Kool, model 12D), which was then cooled to −15 °C and maintained at that temperature. The ambient relative humidity was around 60−70% at room temperature.

As shown in Figure 1, frost formation was much faster on the microtextured surface (Figure 1d) compared to all other morphologies with almost the entire sample covered in the first 5 min. The large surface area due to the presence of

**Received:** January 27, 2016
**Accepted:** May 6, 2016
**Published:** May 6, 2016





DOI: 10.1021/acsami.6b01133
ACS Appl. Mater. Interfaces 2016, 8, 12583−12587

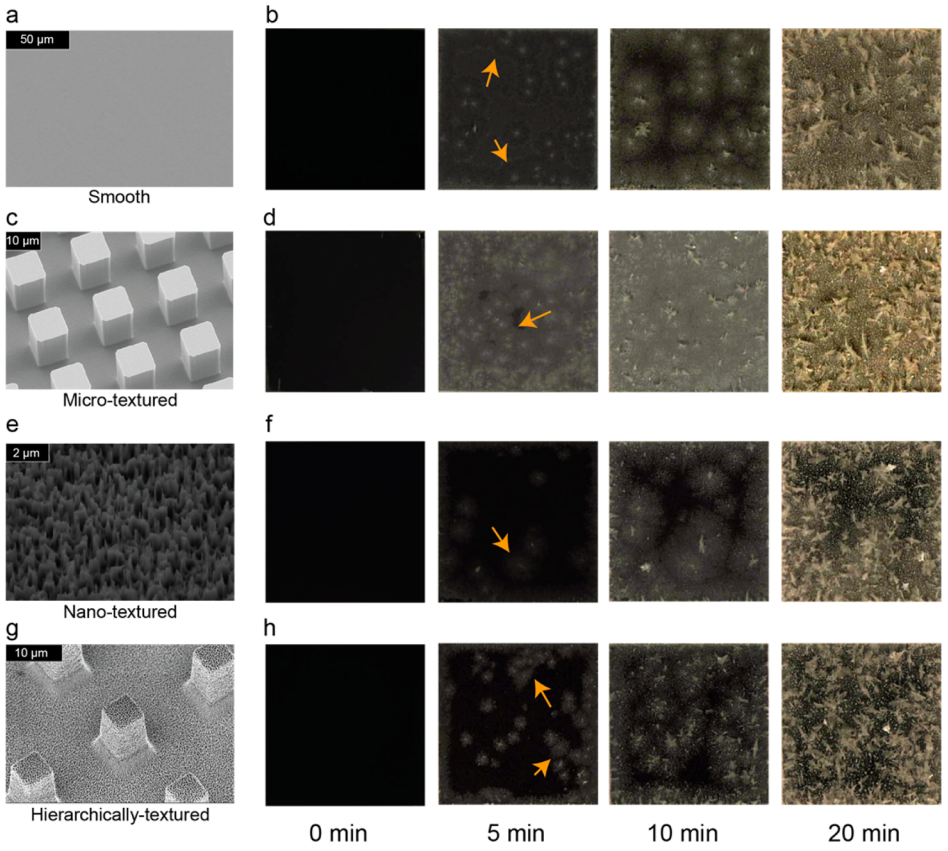


**Figure 1.** SEM images and snapshots of the video showing frost formation at different time instants for a (a, b) smooth hydrophobic surface, (c, d) microtextured superhydrophobic surface, (e, f) nanotextured superhydrophobic surface, and (g, h) hierarchical superhydrophobic surface. The arrows in the snapshots indicate the frost front on the different surfaces.

**Table 1. Dynamic Contact Angles of Water**

| | advancing angle (deg) | receding angle (deg) | contact angle hysteresis (deg) |
|---|---|---|---|
| smooth hydrophobic | 113 ± 1 | 97 ± 1 | ~16 |
| microtextured superhydrophobic | 162 ± 2 | 136 ± 2 | ~26 |
| nanotextured superhydrophobic | 168 ± 4 | 160 ± 2 | ~8 |
| hierarchically textured superhydrophobic | >170 | >170 | negligible |

microfeatures increases the rate of frost formation on this surface. On the nanotextured surface (Figure 1f) and the hierarchically textured surface (Figure 1h), despite larger surface areas, there was a slight delay in frost formation—an observation that requires further investigation. However, the frost front originating from the edges eventually advanced to cover the entire sample across all morphologies. With complete frost coverage, anti-icing characteristics such as droplet repellency and freezing delay are compromised on all surfaces.

Frost formation within the surface features has also been reported to increase ice adhesion strength,[17] although the effect of different surface morphologies on ice adhesion has not been explored. We measured the ice adhesion strength on the different superhydrophobic surfaces used in this work: smooth, microtextured, nanotextured, and hierarchically textured. The substrates were clamped to a base plate and plastic cuvettes of 1 cm × 1 cm cross-section filled with water were inverted on them. The system was cooled to −15 °C using a Peltier cooler (TECA Corporation, model LHP-800CP) and maintained at that temperature for approximately 2 h. A force transducer (Imada, model ZP-44) was used to fracture the interface between ice and the substrate, and the maximum force required to do so was recorded. This force was normalized with the cross-section of the cuvette to give us the adhesion strength of ice on the substrate. The details of the experimental setup are provided elsewhere.[4] Water in the cuvettes increases the local humidity near the substrates and results in frost formation within the surface features. During frost formation, the ice adhesion strength is expected to increase, and any adhesion measurement setup using a water column should take into account the effect of frost formation within the interstitial regions of the surface.

Figure 2 shows the ice adhesion strength expressed as a fraction of that on untreated surfaces. The highest adhesion strength was recorded on microtextured superhydrophobic surfaces with the measured values being higher than even that on untreated surfaces. In comparison, hierarchically textured surfaces showed lower ice adhesion, although its adhesion strength was still higher than what we measured on smooth hydrophobic surfaces. We did not observe any degradation of the silane coating during our experiment (see the Supporting Information). We attribute the high ice adhesion to the indiscriminate frost formation within the air pockets of the microtextured and hierarchically textured surfaces, which modifies the surface properties and leads to "Wenzel ice".[17]

However, ice adhesion strength on nanotextured superhydrophobic surfaces was approximately 15 times lower than that on untreated surfaces and approximately 5 times lower than that on smooth hydrophobic surfaces. Although low ice


DOI: 10.1021/acsami.6b01133
ACS Appl. Mater. Interfaces 2016, 8, 12583−12587

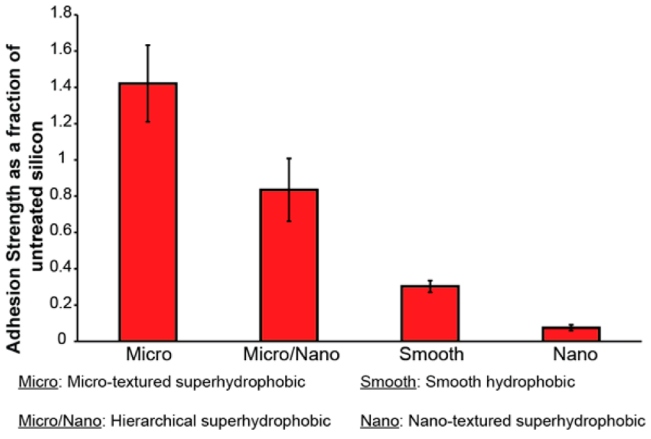


**Figure 2.** Adhesion strength of ice on different surfaces expressed as a fraction of that on untreated silicon.

adhesion on superhydrophobic surfaces under dry conditions has been reported in the past, low ice adhesion under humid conditions has not been previously reported. This result runs contrary to the measurements on other textured superhydrophobic surfaces, indicating the dependence of ice adherence on the surface morphology. The low adherence on nanotextured surfaces suggests a "Cassie" nature of ice in contrast to the "Wenzel" nature of ice on the microtextured and hierarchically textured surfaces. Our observations are consistent with the observations of Maitra et al.,[25] who noted a higher ice adhesion for the hierarchically textured surfaces compared to that for the single scale nanotextured surfaces under concurrent ice shedding. The smaller length scales of the features on nanotextured surfaces could prevent frost formation in the air pockets, thereby preserving the low water wettability and low ice adhesion on these surfaces.

We visualized the formation of frost within the surface features in an SEM via a cryo-fracturing approach. The schematic in Figure 3a outlines the steps involved in this process. Initially, the substrate was cooled on a cold plate (Stir-Kool 12D) and maintained at −15 °C for approximately 15 min (step I). Once a significant amount of frost was seen on the surface, the substrate was plunged into liquid nitrogen (step II) and clamped vertically onto a stage that was maintained at −150 °C. The clamping was done in such a way that a part of the sample protruded from the stage as shown in step III in Figure 3a. The substrate was then broken using a knife (step IV) so that the fractured edge could be imaged in an SEM at cryogenic temperatures (step V).

Figure 3b shows SEM images of the frost formation on a microtextured superhydrophobic surface using the cryo-fracture process. Consistent with earlier works,[17] a significant amount of frost was seen between the textures, rendering the surface hydrophilic. Ice that subsequently forms on the surface will be completely impaled on the surface features, resulting in increased ice adhesion. Similarly, on the hierarchically textured surface, the formation of frost between the micropillars compromises the ice-repellency of the surface and thus increases ice adhesion (Figure 3c).

Imaging the frost−substrate interface on a nanotextured surface was much more challenging. Although there was complete frost coverage prior to the fracturing of the substrate, the destructive cryo-fracturing process removed all the frost crystals from the surface (Figure 3d). Multiple trials similarly failed to obtain a stable frost−substrate interface. Although the poor adherence leading to an unstable frost−substrate interface indicates an absence of frost nucleation in the air pockets, we need a more conclusive imaging technique to visualize the interface and confirm this hypothesis.

Focused ion beam (FIB) milling and subsequent SEM imaging under cryogenic conditions has been used extensively

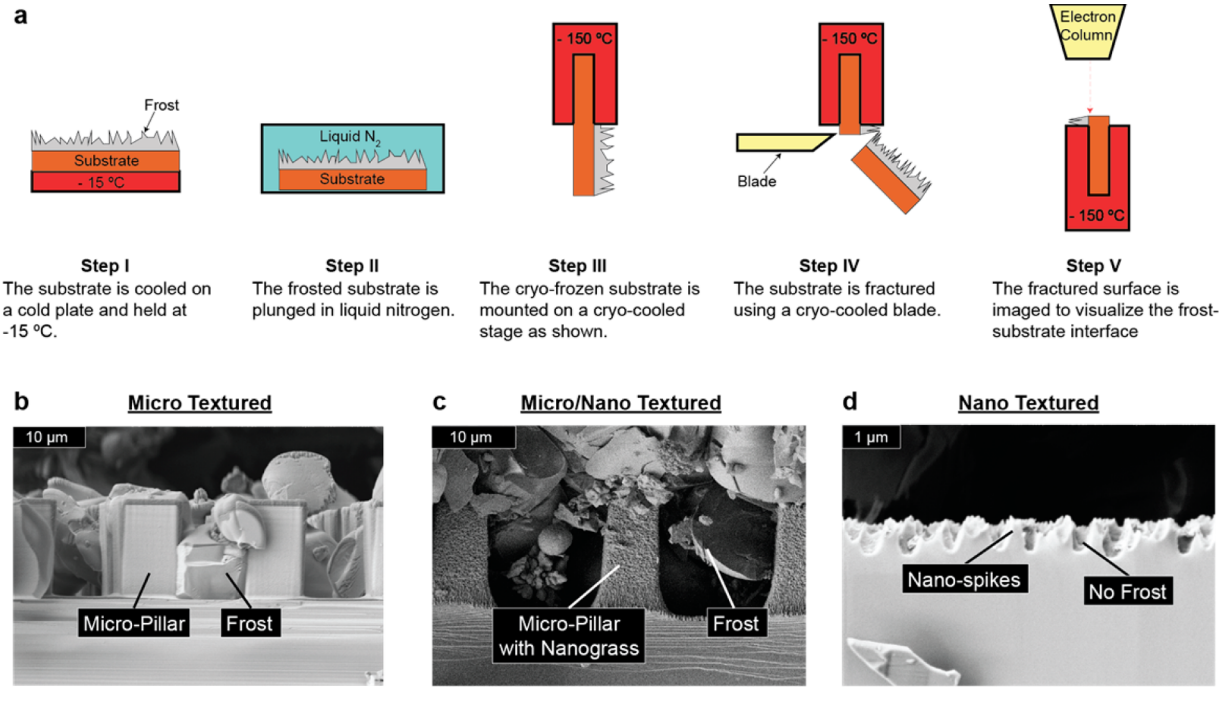


**Figure 3.** (a) Schematic of the steps for cryo fracture/SEM imaging. SEM images of a cryo-fractured (b) microtextured superhydrophobic surface, (c) hierarchically textured superhydrophobic surface, and (d) nanotextured superhydrophobic surface.


DOI: 10.1021/acsami.6b01133
ACS Appl. Mater. Interfaces 2016, 8, 12583−12587

in recent years to characterize surfaces and interfaces at the micro- and nanoscale.[7,26] In this work, we used cryo-FIB/SEM to enable direct visualization of the interface between frost and the nanotextured surface. The substrate was initially maintained at −15 °C at a humidity of around 60−70% at room temperature for approximately 15 min during which a good amount of frost formed on the surface. The substrate was then plunged in liquid nitrogen and mounted onto a cold stage that was cooled to −150 °C in vacuum. The rapid decrease in temperature due to the liquid nitrogen plunge prevented any further deformation prior to imaging. A Pt/Pd coating was applied to the substrate to ensure uniform milling. The substrate was then put in a Zeiss NVision Focused Ion Beam system with dual ion and electron beams as shown in Figure 4a.

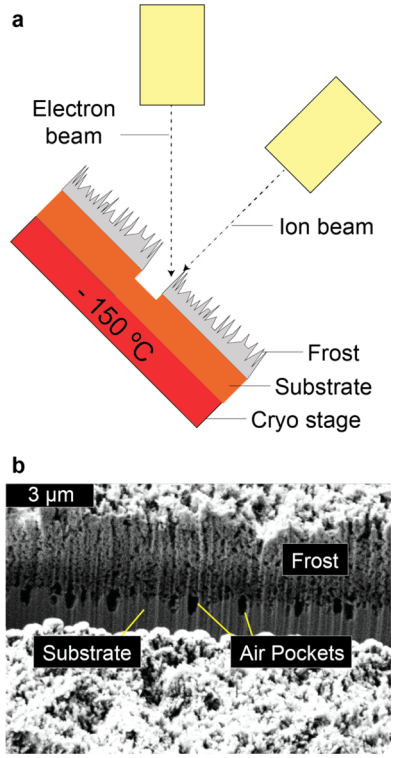


**Figure 4.** (a) Schematic of the cryo-FIB/SEM process. (b) SEM image of the FIB cross-section of the interface between frost and the nanotextured surface.

The gallium ion beam was used to mill through the sample such that the interface between frost and the nanotextured surface was revealed, which was then imaged using the electron beam. Figure 4b shows the SEM image of the cross section of the interface. The image shows the presence of a number of stable air pockets on the nanotextured surface even under high humidity conditions. The nanotextured superhydrophobic surfaces could thus stabilize ice in a suspended "Cassie" state that translates to the low ice adhesion strength reported on these surfaces. There have been other works in the field that have looked at using nanotexturing for frost resistance.[20−22,27] The "Cassie" nature of frost had been hypothesized to be responsible for the favorable defrosting performance of nanotextured superhydrophobic surfaces,[22] but direct visual evidence had not been available before now.

The lack of frost formation in the cavities of the nanotextured surfaces can be explained via the Kelvin equation. It has been shown previously that the vapor phase is stabilized in hydrophobic nanocavities.[28−30] Because of the unavailability of data for the interfacial energy of the frost−vapor interface, we use here the analogy of a liquid−vapor system in a nanocavity. From the Kelvin equation, the equilibrium vapor pressure $P'_{(a)}$ in a cavity of size '$a$' near the surface of a condensed liquid phase is given by

$$P'_{(a)} = P'_{(\infty)}\exp\left(-\frac{4\sigma V''\cos\theta}{aRT}\right) \quad (1)$$

where $P'_{(\infty)}$ is the equilibrium bulk vapor pressure outside the nanocavity, $\sigma$ is the surface tension of the liquid, $a$ is the size of the cavity, $\theta$ is the contact angle of the liquid on the walls of the cavity, $V''$ is the molar volume of the liquid phase, and $T$ is the ambient temperature. See the Supporting Information for the derivation of eq 1. From this equation, we note that, as the size of the cavity decreases, the vapor pressure in the nanocavity increases, thereby stabilizing the vapor phase and inhibiting the formation of the condensed liquid phase. Extending this argument to frost formation, we can expect the energy barrier for frost nucleation inside a nanocavity to be much higher compared to that on a flat surface outside the nanocavity. Future works that provide data for the frost−vapor interfacial energy would be helpful in making precise calculations regarding the effect of the size of the cavities on the stabilization of the vapor pockets under frost-forming conditions.

To conclude, we show that varying the morphology of superhydrophobic surfaces fails to prevent frost formation. Whereas high ice adhesion was observed on microtextured superhydrophobic surfaces due to frost formation within the surface features, extremely low ice adhesion strength was measured on nanotextured superhydrophobic surfaces even under conditions of high local humidity. The characteristics of the interface between frost and the substrate play a crucial role in determining the ice adhesion and were investigated here via cryogenic imaging. Whereas frost formation within the surface features on the microtextured and hierarchically textured surfaces leads to the formation of the impaled "Wenzel ice", the presence of stable air pockets on the nanotextured surface even under frosting conditions stabilizes "Cassie ice" on the surface. These observations can help us establish the critical length scale required to promote "Cassie ice" and take us a step closer to designing feasible and effective anti-icing surfaces.

## ■ ASSOCIATED CONTENT

### Supporting Information

The Supporting Information is available free of charge on the ACS Publications website at DOI: 10.1021/acsami.6b01133.

Durability of the silane-treated surfaces during the experiment and derivation of the Kelvin equation for water−water vapor equilibrium in a hydrophobic nanocavity (PDF)

## ■ AUTHOR INFORMATION

### Corresponding Author

*E-mail: varanasi@mit.edu.

### Notes

The authors declare no competing financial interest.

## ■ ACKNOWLEDGMENTS

We thank Nicholas Antoniou and Adam Graham at the Center for Nanoscale Systems, Harvard University for their extensive



DOI: 10.1021/acsami.6b01133
ACS Appl. Mater. Interfaces 2016, 8, 12583−12587

help during the cryogenic imaging. We also acknowledge Seyed Reza Mahmoudi for his valuable inputs during the discussions.

## REFERENCES

(1) Sayward, J. M. *Seeking Low Ice Adhesion*; The Laboratory: Hanover, New Hampshire, USA, 1979.
(2) Laforte, J. L.; Allaire, M. a.; Laflamme, J. State-of-the-Art on Power Line de-Icing. *Atmos. Res.* **1998**, *46*, 143−158.
(3) Ramakrishna, D. M.; Viraraghavan, T. Environmental Impact of Chemical Deicers − A Review. *Water, Air, Soil Pollut.* **2005**, *166*, 49−63.
(4) Meuler, A. J.; Smith, J. D.; Varanasi, K. K.; Mabry, J. M.; McKinley, G. H.; Cohen, R. E. Relationships between Water Wettability and Ice Adhesion. *ACS Appl. Mater. Interfaces* **2010**, *2* (11), 3100−3110.
(5) Kulinich, S. A.; Farzaneh, M. Ice Adhesion on Super-Hydrophobic Surfaces. *Appl. Surf. Sci.* **2009**, *255* (18), 8153−8157.
(6) Cao, L.; Jones, A. K.; Sikka, V. K.; Wu, J.; Gao, D. Anti-Icing Superhydrophobic Coatings. *Langmuir* **2009**, *25* (21), 12444−124488.
(7) Subramanyam, S. B.; Rykaczewski, K.; Varanasi, K. K. Ice Adhesion on Lubricant-Impregnated Textured Surfaces. *Langmuir* **2013**, *29* (44), 13414−13418.
(8) Kim, P.; Wong, T.-S.; Alvarenga, J.; Kreder, M. J.; Adorno-Martinez, W. E.; Aizenberg, J. Liquid-Infused Nanostructured Surfaces with Extreme Anti-Ice and Anti-Frost Performance. *ACS Nano* **2012**, *6* (8), 6569−6577.
(9) Mishchenko, L.; Hatton, B.; Bahadur, V.; Taylor, J. A.; Krupenkin, T.; Aizenberg, J. Design of Ice-Free Nanostructured Surfaces Based on Repulsion of Impacting Water Droplets. *ACS Nano* **2010**, *4* (12), 7699−7707.
(10) Maitra, T.; Tiwari, M. K.; Antonini, C.; Schoch, P.; Jung, S.; Eberle, P.; Poulikakos, D. On the Nanoengineering of Super-hydrophobic and Impalement Resistant Surface Textures below the Freezing Temperature. *Nano Lett.* **2014**, *14* (1), 172−182.
(11) Tourkine, P.; Le Merrer, M.; Quéré, D. Delayed Freezing on Water Repellent Materials. *Langmuir* **2009**, *25* (13), 7214−7216.
(12) Eberle, P.; Tiwari, M. K.; Maitra, T.; Poulikakos, D. Rational Nanostructuring of Surfaces for Extraordinary Icephobicity. *Nanoscale* **2014**, *6* (9), 4874−4881.
(13) Jung, S.; Dorrestijn, M.; Raps, D.; Das, A.; Megaridis, C. M.; Poulikakos, D. Are Superhydrophobic Surfaces Best for Icephobicity? *Langmuir* **2011**, *27*, 3059−3066.
(14) Fang, G.; Amirfazli, A. Understanding the Anti-Icing Behavior of Superhydrophobic Surfaces. *Surf. Innovations* **2014**, *2* (2), 94−102.
(15) Farhadi, S.; Farzaneh, M.; Kulinich, S. A. Anti-Icing Performance of Superhydrophobic Surfaces. *Appl. Surf. Sci.* **2011**, *257* (14), 6264−6269.
(16) Quéré, D. Wetting and Roughness. *Annu. Rev. Mater. Res.* **2008**, *38* (1), 71−99.
(17) Varanasi, K.; Deng, T.; Smith, J.; Hsu, M.; Bhate, N. Frost Formation and Ice Adhesion on Superhydrophobic Surfaces. *Appl. Phys. Lett.* **2010**, *97* (23), 234102.
(18) Kulinich, S. A.; Farhadi, S.; Nose, K.; Du, X. W. Super-hydrophobic Surfaces: Are They Really Ice-Repellent? *Langmuir* **2011**, *27* (1), 25−29.
(19) Jung, S.; Tiwari, M. K.; Poulikakos, D. Frost Halos from Supercooled Water Droplets. *Proc. Natl. Acad. Sci. U. S. A.* **2012**, *109* (40), 16073−16078.
(20) He, M.; Wang, J.; Li, H.; Jin, X.; Wang, J.; Liu, B.; Song, Y. Super-Hydrophobic Film Retards Frost Formation. *Soft Matter* **2010**, *6* (11), 2396−2399.
(21) Boreyko, J. B.; Collier, C. P. Delayed Frost Growth on Jumping-Drop Superhydrophobic Surfaces. *ACS Nano* **2013**, *7* (2), 1618−1627.
(22) Boreyko, J. B.; Srijanto, B. R.; Nguyen, T. D.; Vega, C.; Fuentes-Cabrera, M.; Collier, C. P. Dynamic Defrosting on Nanostructured Superhydrophobic Surfaces. *Langmuir* **2013**, *29* (30), 9516−9524.
(23) Petit, J.; Bonaccurso, E. General Frost Growth Mechanism on Solid Substrates with Different Stiffness. *Langmuir* **2014**, *30* (4), 1160−1168.
(24) Anand, S.; Paxson, A. T.; Dhiman, R.; Smith, J. D.; Varanasi, K. K. Enhanced Condensation on Lubricant-Impregnated Nanotextured Surfaces. *ACS Nano* **2012**, *6* (11), 10122−10129.
(25) Maitra, T.; Jung, S.; Giger, M. E.; Kandrical, V.; Ruesch, T.; Poulikakos, D. Superhydrophobicity vs. Ice Adhesion: The Quandary of Robust Icephobic Surface Design. *Adv. Mater. Interfaces* **2015**, *2* (16), 1500330.
(26) Rykaczewski, K.; Landin, T.; Walker, M. L.; Scott, J. H. J.; Varanasi, K. K. Direct Imaging of Complex Nano- to Microscale Interfaces Involving Solid, Liquid, and Gas Phases. *ACS Nano* **2012**, *6* (10), 9326−9334.
(27) Chen, X.; Ma, R.; Zhou, H.; Zhou, X.; Che, L.; Yao, S.; Wang, Z. Activating the Microscale Edge Effect in a Hierarchical Surface for Frosting Suppression and Defrosting Promotion. *Sci. Rep.* **2013**, *3*, 2515.
(28) Zargarzadeh, L.; Elliott, J. A. W. Surface Thermodynamic Analysis of Fluid Confined in a Cone and Comparison with the Sphere−Plate and Plate−Plate Geometries. *Langmuir* **2013**, *29* (42), 12950−12958.
(29) Jones, P. R.; Hao, X.; Cruz-Chu, E. R.; Rykaczewski, K.; Nandy, K.; Schutzius, T. M.; Varanasi, K. K.; Megaridis, C. M.; Walther, J. H.; Koumoutsakos, P.; Espinosa, H. D.; Patankar, N. A. Sustaining Dry Surfaces under Water. *Sci. Rep.* **2015**, *5*, 12311.
(30) Patankar, N. a. Supernucleating Surfaces for Nucleate Boiling and Dropwise Condensation Heat Transfer. *Soft Matter* **2010**, *6* (8), 1613−1620.


DOI: 10.1021/acsami.6b01133
*ACS Appl. Mater. Interfaces* 2016, 8, 12583−12587